ChemPubSoc Europe

DOI: 10.1002/cphc.201600663

CHEMPHYSCHEM Communications

Limits in Proton Nuclear Singlet-State Lifetimes Measured with *para*-Hydrogen-Induced Polarization

Yuning Zhang[+],[a] Xueyou Duan[+],[a] Pei Che Soon,[a] Vladimír Sychrovský,[b, c] James W. Canary,*[a] and Alexej Jerschow*[a]

The synthesis of a hyperpolarized molecule was developed, where the polarization and the singlet state were preserved over two controlled chemical steps. Nuclear singlet-state lifetimes close to 6 min for protons are reported in dimethyl fumarate. Owing to the high symmetry ($AA'X_3X_3'$ and A_2 systems), the singlet-state readout requires either a chemical desymmetrization or a long and repeated spin lock. Using DFT calculations and relaxation models, we further determine nuclear spin singlet lifetime limiting factors, which include the intramolecular dipolar coupling mechanism (proton–proton and proton–deuterium), the chemical shift anisotropy mechanism (symmetric and antisymmetric), and the intermolecular dipolar coupling mechanism (to oxygen and deuterium). If the limit of paramagnetic relaxation caused by residual oxygen could be lifted, the intramolecular dipolar coupling to deuterium would become the limiting relaxation mechanism and proton lifetimes upwards of 26 min could become available in the molecules considered here (dimethyl maleate and dimethyl fumarate).

Over the last several years, it has been established that nuclear spin singlet states can have lifetimes of up to several orders of magnitude longer than the longitudinal relaxation time T_1.[1] The most impressive results to date have been achieved for ^{15}N and ^{13}C spin singlets, where lifetimes of 23–26 min and more than 1 h were reported,[1c,e,2] respectively. Owing to the high gyromagnetic ratio γ, proton spins are inherently more prone to singlet-breaking mechanisms, and we thus investigated what the limiting lifetimes might be for proton spins in organic molecules of high symmetry. Such questions are important when applications of hyperpolarization are considered for contrast agents, for example, or in cases where long-term storage of magnetization would be desired. It is also of interest whether weaker relaxation mechanisms can be measured and exploited for structural or dynamical characterization.

para-Hydrogen-induced polarization enhancement (PHIP) can provide polarization enhancements of up to several thousand times through the hydrogenation of a molecule with a *para*-H_2-enriched gas,[3] or through the transfer of magnetization in an intermediate complex, without the addition of H_2 to the molecule.[4] The enhanced polarization could, in principle, be stored in a nuclear singlet state for later readout. Although transfer of the polarization to low-γ nuclei is of interest, owing to the longer T_1 times, storage directly in the proton spins is desirable as well, especially for certain imaging applications.[6] Inherent symmetry in the molecules of study can reduce the action of major relaxation mechanisms[7] (such as certain dipolar coupling interactions, the chemical shift anisotropy,[8] and singlet–triplet leakage), but symmetry alone does not guarantee long lifetimes.[8]

In this work, our goal was to study the proton singlet lifetimes of organic molecules in solution with increased degrees of magnetic equivalence, including a molecule with an inversion center. The increased symmetry requires the use of special readout techniques, which include field cycling,[9] pulse sequences,[3c,7a,b,10] and chemical reactions.[7d,11] We have previously demonstrated a chemical readout method based on a bio-inspired thiol-addition reaction, which can desymmetrize the molecule and can, thus, reveal the singlet signals.[11b] Another approach is based on a weak spin lock (SLIC),[7b,c,10a,b] which we have adapted to the readout of singlet states under weak chemical inequivalence[12] with a multiple readout method.[3c] Both of these techniques, as well as the PHIP enhancement, are essential for accessing the singlet states in the molecules of study, which would otherwise remain invisible. Multiconfiguration ab initio calculations provide a means for calculating dipolar coupling and chemical-shift relaxation contributions to the singlet lifetime limits.

We present here results on the vinylene proton singlets of the dimethyl maleate (DMM) and dimethyl fumarate (DMF) molecules. DMF is currently an important, commercially available pharmaceutical.[13] We obtained its hyperpolarized version from PHIP-prepared DMM through isomerization with a secondary amine.[14] The singlet state of the DMM was preserved in DMF despite the low symmetry of the intermediate.

Both DMM and DMF form nearly equivalent $AA'X_3X'_3$ systems (with A denoting the vinylene protons and X the methyl pro-

[a] *Y. Zhang,[+] X. Duan,[+] Dr. P. C. Soon, Prof. J. W. Canary, Prof. A. Jerschow*
Department of Chemistry
New York University
100 Washington Sq. East, New York, NY 10003 (USA)
E-mail: james.canary@nyu.edu
alexej.jerschow@nyu.edu

[b] *Dr. V. Sychrovský*
Institute of Organic Chemistry and Biochemistry
Academy of Sciences of the Czech Republic, v.v.i.
Flemingovo náměstí 2, 166 10, Praha 6 (Czech Republic)

[c] *Dr. V. Sychrovský*
Department of Electrotechnology, Electrical Engineering
Czech Technical University
Technická 2, 166 27, Prague 6 (Czech Republic)

[+] *These authors contributed equally to this work*

Supporting Information for this article can be found under: http://dx.doi.org/10.1002/cphc.201600663.

tons—compounds **2a** and **3a**, respectively), or effective A_2 systems when the methyl groups are deuterated (compounds **2b** and **3b**). The inequivalence in compounds **2b** and **3b** was estimated to be below 0.06 Hz from the experimentally determined ^1H–^1H *J* coupling (0.4 Hz), by scaling with the relative gyromagnetic ratio. The high degree of symmetry does not allow one to initialize the molecule with a non-thermal singlet state, but the addition of *p*-H_2 in a PHIP step is used to perform this task. The DMF-d_6 molecule provides the highest degree of symmetry of the series considered here, with an inversion center between the vinylene protons.

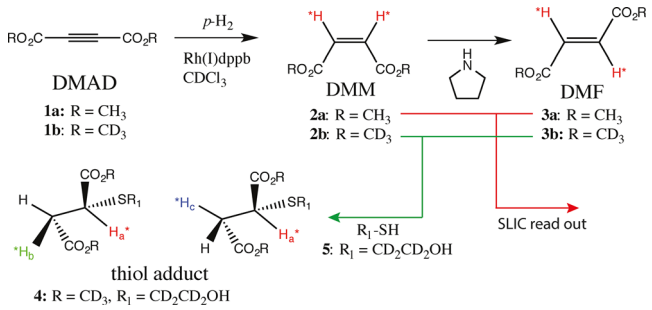

Figure 1. Reaction scheme: **1** was hydrogenated with *p*-H_2 to yield **2** followed by an isomerization reaction with pyrrolidine to generate **3**. Singlets in **2a** or **3a** were read out by a weak spin lock (SLIC, red arrow), and those in **2b** or **3b** were read out by adding **5** (green arrow). Hyperpolarized signals of H_a*, H_b*, and H_c* in thiol adduct **4** were acquired through OPSY.[5]

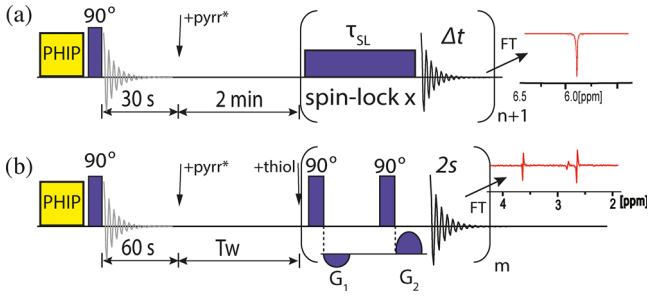

Figure 2. Pulse sequences and experimental procedures: a) multi-SLIC readout method. PHIP is initiated at earth field, after which the sample is placed in the magnet and a 90° spoiler pulse is initiated. After 30 s, pyrrolidine is added for the isomerization reaction when DMF (**3a** or **3b**) is measured, or a dummy solution ($CDCl_3$) when measuring DMM (**2a** or **2b**). After 2 min, the multi-SLIC is applied, resulting in a negative in-phase SLIC peak. b) Chemical reaction readout sequence. The signals are read out by using multiple OPSY modules (yielding antiphase peaks). The distinct shifts and number of peaks relative to (a) are attributed to the chemical desymmetrization from thiol addition, as needed for the OPSY readout (see also Figure S6).

The reaction procedure is illustrated in Figure 1, and the associated pulse sequences are shown in Figure 2. After hyperpolarization using PHIP and placing the sample into the magnet (11.76 T), the signals were allowed to decay for a constant period of time. Injection of pyrrolidine was used to convert DMM to DMF, and after an additional delay to allow the reaction to complete (2 min), the readout was performed either through chemical desymmetrization (for **2a**/**3a**) or with a multiple SLIC readout (for **2b**/**3b**); see the Supporting Information for sequence and spectral details. For the chemical desymmetrization readout, a thiol solution was injected, and the signals were subsequently recorded by using an OPSY (only *para*-hydrogen spectroscopy)[5] sequence as a function of the waiting period T_w. OPSY uses a double-quantum filter to yield a spectrum selective only for sites enhanced by *para*-hydrogen. The OPSY readout was repeated at 2 s intervals until the reaction was complete. For the multi-SLIC readout, the detection sequence was initiated 2 min after pyrrolidine injection, and the signal was recorded as a function of the delay, Δt. The analysis of the decay in subsequent readouts as a function of Δt allows one to deduce the signal lifetime and the conversion rate.[3c,12] To ensure an accurate comparison, the procedure for DMM was performed in exactly the same way, except that the first injection solution did not contain pyrrolidine. All solutions were thoroughly degassed to remove oxygen. Typical spectra observed with SLIC and OPSY are shown in red in Figure 2.

For SLIC, the nutation frequency was optimal at 11.6 Hz for **2a** and 18.0 Hz for **3a**, and the pulse was applied on-resonance with the vinylene protons. These nutation rates should correspond to the vinylene proton coupling constants.[7b,c,10a,b] The duration of the spin lock (τ_{SL}) was optimal at 1.77 s for both compounds, indicating that the difference between the out-of-pair couplings was approximately 0.4 Hz in both cases.

The results of the different T_1 and singlet-state lifetime (T_S) measurements are shown in Table 1. The longest T_S was observed for DMF-d_6 (**3b**), where it reached a value larger than 5.8 min (Figure 3). For DMM-d_6, the singlet lifetime is somewhat shorter (ca. 5.5 min), but the factor relative to T_1 is significantly larger (T_S is longer by a factor of over 17 for **2b**). This observation points to the fact that there is a significant relaxation mechanism limiting the DMF lifetime, which otherwise could be much longer.

Table 1. Summary of measured and calculated R_1 and R_S values for DMM (**2a**, **2b**) and DMF (**3a**, **3b**). All values are given in units of $10^{-3}\,s^{-1}$ (see Table S2 in the Supporting Information for the corresponding time constants).

Parameter [$10^{-3}\,s^{-1}$]	DMM **2a**	DMM-d_6 **2b**	DMF **3a**	DMF-d_6 **3b**
Experimental				
R_1	58.70	53.65	21.49	14.40
R_S	4.50	3.04	6.59	2.86
Calculated				
R_S^{S-T}	0.083	0.012[a]	0.013	0.002[a]
$R_S^{D,intra}$	2.14	0.134[a]	10.10	0.635[a]
$R_S^{\Delta\sigma^+}$	0.351	0.351	< 0.0001	< 0.0001
$R_S^{\Delta\sigma^-}$	0.051	0.051	< 0.001	< 0.001
$R_S^{D,inter}$	0.043[a]	0.043[a]	0.044[a]	0.044[a]
$R_S^{O_2,para}$	5.45	5.45	4.87	4.87

[a] H–D scalar/dipolar coupling considered.

A computational analysis of different relaxation mechanisms was performed to examine the relative magnitudes of different relaxation mechanisms. The calculation of internuclear distances and NMR parameters was performed by using a configurational average over low-lying energy states, arising from methyl rotations.

The DFT calculations revealed that the global energy minimum of DMM represented a twisted conformation, which was approximately 9.3 kcal mol^{-1} lower in energy compared to the energy of planar symmetric DMM (see the Supporting Information). The twisted structure of DMM resulted in asymmetric distances between the vinylene hydrogen atoms and hydrogen atoms of the methyl groups, with one methyl group almost in-plane and the other out of plane (Figures S7 and S8). Exchange of the twist between the two methyl groups is allowed with a low-energy barrier, and hence there is rapid interchange between the two twists on timescales much faster than the correlation times relevant for NMR relaxation. Therefore, this twist does not in itself lead to inequivalence or enhancement of relaxation. The noted fast motions effectively "symmetrize the molecule" on the NMR timescale. The methyl rotation barrier was approximately 1.9 kcal mol^{-1}. The rotational motion modulated the DMM structure and J couplings negligibly (Table S1). DMF, by contrast, did not show significant excursions from a planar conformation, and this behavior remained conserved upon methyl rotation.

Configurational averaging was performed before calculating relaxation rates. This procedure provided a means of averaging the methyl rotation motion and conversions between configurations, which both occur at timescales much faster than the molecular correlation time. Further details are given in the Supporting Information.

The calculated J couplings generally followed the trend seen in the experiments ($J_V = 14.5$ Hz and $|J_{VM} - J_{VM'}| = 0.30$ Hz for DMM, whereas $J_V = 17.3$ Hz and $|J_{VM} - J_{VM'}| = 0.04$ Hz for DMF), where the couplings were averaged over chemically identical pairs (Figure S10).

The total singlet-state relaxation rate R_S is given by Equation (1):

$$R_S = R_S^{S-T} + R_S^{D,intra} + R_S^{\Delta\sigma^+} + R_S^{\Delta\sigma^-} + R_S^{D,inter} + R_S^{O_2,para} + R_S^{other} \quad (1)$$

where the different terms correspond to singlet–triplet leakage (R_S^{S-T}), intramolecular dipolar relaxation ($R_S^{D,intra}$), the symmetric and antisymmetric chemical shift anisotropy (CSA) mechanisms ($R_S^{\Delta\sigma^+}$ and $R_S^{\Delta\sigma^-}$), intermolecular dipolar relaxation ($R_S^{D,inter}$), paramagnetic relaxation owing to oxygen ($R_S^{O_2,para}$), and an unknown remaining contribution (R_S^{other}).

Singlet–triplet leakage rates R_S^{S-T} represent the coherent evolution out of the singlet state (owing to inequivalence) coupled with a T_1 relaxation process. These rates were estimated as described previously,[11b] using the measured coupling and relaxation values (see also the Supporting Information). As shown in Table 1, this mechanism can be neglected (the lifetimes from this mechanism would exceed 20 h for **2b** and 130 h for **3b**).

For the calculation of the intramolecular dipolar and CSA relaxation mechanism contributions, rigid molecular tumbling was assumed. The overall molecular tumbling correlation times τ_c were determined as 17.8 and 21.8 ps for DMM and DMF, respectively, from the intramolecular dipolar relaxation contributions to the experimental T_1 values by using the calculated and configurationally averaged internuclear distances.

By using these τ_c values and configurational averaging, the intramolecular dipolar contribution to the singlet-state relaxation rate $R_S^{D,intra}$ was calculated by employing the rotational auto- and cross-correlation functions (see the Supporting Information). For deuterated compounds **2b** and **3b**, the rates were calculated by substituting the deuterium gyromagnetic ratios. As expected, the intramolecular dipolar coupling contribution is significantly reduced by methyl deuteration (see values of $R_S^{D,intra}$ for **2b** and **3b**).

The $R_S^{D,intra}$ trends agree qualitatively with the experimental findings, but the calculated rates are larger than the experimental values. For example, looking at the change in observed rates upon deuteration, taking $\Delta R_S = R_S(\mathbf{2b}) - R_S(\mathbf{2a})$, one would obtain the relaxation contribution of only the long-range intramolecular dipolar couplings, which is 1.46×10^{-3} s^{-1}.

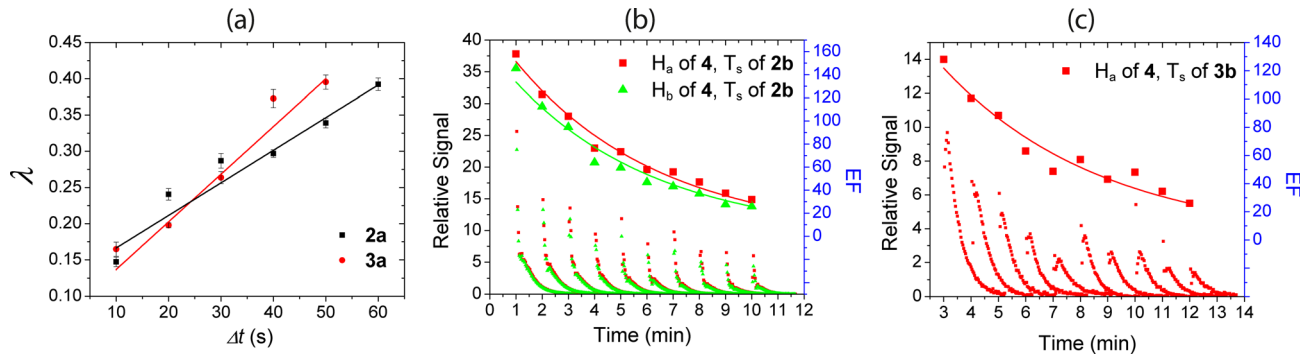

Figure 3. Experimental results: a) the multi-SLIC readout decay rate is plotted against the time interval between readouts and fitted to $\lambda = \frac{1}{T_S}\Delta t - \ln(1-\xi)$, with ξ being the conversion fraction, as described previously.[3c,12] This procedure gives T_S of **2a** (black) as 3.70 ± 0.42 min, and T_S of **3a** (red) as 2.53 ± 0.29 min. b,c) Thiol addition reaction readout results. OPSY signal (normalized to the thermal peak, shown on the left y axis) and enhancement factor (right y axis) of hyperpolarized ^{1}H decays as a function of the waiting period T_w between singlet initiation and injection of thiols for **2b** and **3b**. T_S of **2b** is 5.48 ± 0.29 min. T_S of **3b** is 5.82 ± 0.53 min. The enhancement factor represents the ratio of total signal (as calculated by summing up the signal from the OPSY train) to the corresponding thermal signals.[12]

The theoretical value $\Delta R_S^{D,intra} = R_S^{D,intra}(2\,\mathbf{b}) - R_S^{D,intra}(2\,\mathbf{a})$, is $2.00\times10^{-3}\,s^{-1}$. For DMF, a larger discrepancy $[\Delta R_S^{D,intra} = R_S^{D,intra}(3\,\mathbf{b}) - R_S^{D,intra}(3\,\mathbf{a})]$ is found, with the measured value being $3.73\times10^{-3}\,s^{-1}$ and the calculated amounting to $9.47\times10^{-3}\,s^{-1}$. Part of this discrepancy may be attributed to large side-chain flexibility, which could effectively increase the average distances between the methyl and the vinylene protons, and thus produce a reduced dipolar relaxation contribution.

The contributions to singlet relaxation from chemical-shift anisotropy, $R_S^{\Delta\sigma^+}$ for the symmetric portion and $R_S^{\Delta\sigma^-}$ for the antisymmetric portion, were calculated according to Equations (10) and (11) of Zhang et al.[12] As seen in Table 1, the contribution of this mechanism to the overall R_S is small (a lifetime limit of approximately 47 min would be predicted for **2a** and **2b**), and is de facto absent altogether for DMF, owing to the inversion center symmetry. The magnitude of $R_S^{\Delta\sigma^-}$ is also smaller than that reported previously for DMM,[12] likely as a result of the configurational averaging performed here.

Although the majority of the intermolecular dipolar relaxation mechanisms can be avoided by using a deuterated solvent, there remain interactions with the deuterium spin and dissolved oxygen in solution.[15] The intermolecular dipolar and paramagnetic relaxation contributions from solvent deuterium $(R_S^{D,inter})$ and dissolved oxygen $(R_S^{O_2,para})$ were calculated according to the prescription given by Pileio,[15] which is also summarized in the Supporting Information. The intermolecular relaxation rates for DMM and DMF are very similar to each other. The reason is that the geometrical factors entering the intermolecular relaxation model partially compensate each other (notably, the hydrodynamic radii and the eccentricity parameters, as described in the Supporting Information).

For the paramagnetic mechanism $R_S^{O_2,para}$, the residual oxygen concentration in the mixture was estimated to be 0.2 mM by comparing T_1 measurements with and without degassing and by using the solubility value of oxygen in chloroform (1.82 mM).[16] It is noted that $R_S^{O_2,para}$ rates represent the largest theoretically obtained relaxation rates, and are larger than the experimentally determined ones, except for **3a**. This finding clearly indicates that the measured singlet-state relaxation rates are most likely limited by the paramagnetic relaxation mechanism caused by residual oxygen. This finding is in line with an earlier report of ^1H T_S for an asymmetric maleate diester, 1-(ethyl-d_5),4-(propyl-d_7)(*Z*)-but-2-enedioate, in carefully degassed conditions.[6b] It was subsequently assumed that plastic tubing allowed oxygen to penetrate into the sample region.[6a] An improvement in oxygen removal over our current setup would have to be achieved by a factor of 10–20 to reveal the next biggest contribution to R_S, which is the intramolecular proton deuterium dipolar relaxation $(R_S^{D,intra})$ for DMF-d_6 and the symmetric CSA mechanism $(R_S^{\Delta\sigma^+})$ for DMM-d_6. At this stage, it is not clear whether this is achievable with the multiple-injection procedure, owing to diffusion of oxygen through the tubing. The lifetime limit for **3b** is predicted to be 26 min based on the calculations presented here. Removal of the intramolecular H–D dipolar relaxation mechanism would require deuterium to be replaced by an NMR-inactive isotope. If that mechanism were to be avoided, the next limiting factor would be intermolecular dipolar relaxation $(R_S^{D,inter})$ from solvent deuterium, potentially allowing the observation of lifetimes of up to 380 min.

Finally, we should point out that the term R_S^{other} may include the mechanism of spin-internal motion, as described by Levitt and co-workers,[1e] wherein spins couple to fluctuating fields from certain internal motions. This mechanism has not been considered here, because it has not been fully formalized yet. The ability to measure long singlet lifetimes, however, provides a potential tool for examining this and other unknown mechanisms.

In summary, we have investigated proton nuclear spin singlet-state lifetimes of small and symmetric organic molecules. It is shown that inversion symmetry does not directly allow one to observe extremely long singlet lifetimes, owing to intermolecular paramagnetic relaxation from oxygen and intramolecular relaxation due to deuterium. The measurements were enabled by hyperpolarization through PHIP and a subsequent polarization- and singlet-preserving isomerization reaction, followed by chemical desymmetrization. The presence of an inversion center allows one to remove contributions of CSA relaxation,[1d] which could be important, in particular, in the slow motion regime (e.g. in high-viscosity solvents or with larger molecules). The preparation of hyperpolarized dimethyl fumarate, as described in this work, could be an important step in the study of its pharmacological properties.

Acknowledgements

This work was supported by US National Science Foundation (NSF) grants CHE-1412568 (J.C.) and CHE-0957586 (A.J.), as well as the Margaret and Herman Sokol Doctoral Fellowship 2014–2015 (Y.Z.). The authors would like to acknowledge Kaustabh Basu for help with degassing and injection procedures.

Keywords: chemical shift anisotropy · dimethyl fumarate · hyperpolarization · paramagnetic relaxation · singlet lifetime limits

[1] a) M. Carravetta, O. G. Johannessen, M. H. Levitt, *Phys. Rev. Lett.* **2004**, *92*, 153003; b) M. H. Levitt, *Annu. Rev. Phys. Chem.* **2012**, *63*, 89–105; c) G. Pileio, M. Carravetta, E. Hughes, M. H. Levitt, *J. Am. Chem. Soc.* **2008**, *130*, 12582–12583; d) G. Pileio, J. T. Hill-Cousins, S. Mitchell, I. Kuprov, L. J. Brown, R. C. D. Brown, M. H. Levitt, *J. Am. Chem. Soc.* **2012**, *134*, 17494–17497; e) G. Stevanato, J. T. Hill-Cousins, P. Hakansson, S. S. Roy, L. J. Brown, R. C. D. Brown, G. Pileio, M. H. Levitt, *Angew. Chem. Int. Ed.* **2015**, *54*, 3740–3743; *Angew. Chem.* **2015**, *127*, 3811–3814.

[2] a) T. Theis, G. X. Ortiz, Jr., A. W. Logan, K. E. Claytor, Y. Feng, W. P. Huhn, V. Blum, S. J. Malcolmson, E. Y. Chekmenev, Q. Wang, W. S. Warren, *Sci. Adv.* **2016**, *2*, e1501438.

[3] a) C. R. Bowers, D. P. Weitekamp, *Phys. Rev. Lett.* **1986**, *57*, 2645–2648; b) C. R. Bowers, D. P. Weitekamp, *J. Am. Chem. Soc.* **1987**, *109*, 5541–5542; c) M. B. Franzoni, D. Graafen, L. Buljubasich, L. M. Schreiber, H. W. Spiess, K. Munnemann, *Phys. Chem. Chem. Phys.* **2013**, *15*, 17233–17239.

[4] R. W. Adams, J. A. Aguilar, K. D. Atkinson, M. J. Cowley, P. I. P. Elliott, S. B. Duckett, G. G. R. Green, I. G. Khazal, J. Lopez-Serrano, D. C. Williamson, *Science* **2009**, *323*, 1708–1711.

[5] J. A. Aguilar, P. I. P. Elliott, J. Lopez-Serrano, R. W. Adams, S. B. Duckett, *Chem. Commun.* **2007**, 1183 – 1185.
[6] a) G. Pileio, J. N. Dumez, I. A. Pop, J. T. Hill-Cousins, R. C. D. Brown, *J. Magn. Reson.* **2015**, *252*, 130 – 134; b) J. N. Dumez, J. T. Hill-Cousins, R. C. Brown, G. Pileio, *J. Magn. Reson.* **2014**, *246*, 27 – 30; c) D. Graafen, M. B. Franzoni, L. M. Schreiber, H. W. Spiess, K. Munnemann, *J. Magn. Reson.* **2016**, *262*, 68 – 72.
[7] a) Y. Feng, R. M. Davis, W. S. Warren, *Nat. Phys.* **2012**, *8*, 831 – 837; b) Y. Feng, T. Theis, T. L. Wu, K. Claytor, W. S. Warren, *J. Chem. Phys.* **2014**, *141*, 134307; c) Y. S. Feng, T. Theis, X. F. Liang, Q. Wang, P. Zhou, W. S. Warren, *J. Am. Chem. Soc.* **2013**, *135*, 9632 – 9635; d) W. S. Warren, E. Jenista, R. T. Branca, X. Chen, *Science* **2009**, *323*, 1711 – 1714.
[8] G. Stevanato, S. S. Roy, J. Hill-Cousins, I. Kuprov, L. J. Brown, R. C. D. Brown, G. Pileio, M. H. Levitt, *Phys. Chem. Chem. Phys.* **2015**, *17*, 5913 – 5922.
[9] M. B. Franzoni, L. Buljubasich, H. W. Spiess, K. Munnemann, *J. Am. Chem. Soc.* **2012**, *134*, 10393 – 10396.
[10] a) S. J. DeVience, R. L. Walsworth, M. S. Rosen, *Phys. Rev. Lett.* **2013**, *111*, 173002; b) T. Theis, Y. Feng, T. Wu, W. S. Warren, *J. Chem. Phys.* **2014**, *140*, 014201; c) G. Pileio, M. Carravetta, M. H. Levitt, *Proc. Natl. Acad. Sci. USA* **2010**, *107*, 17135 – 17139; d) M. C. Tayler, M. H. Levitt, *Phys. Chem. Chem. Phys.* **2011**, *13*, 5556 – 5560.
[11] Y. Zhang, P. C. Soon, A. Jerschow, J. W. Canary, *Angew. Chem. Int. Ed.* **2014**, *53*, 3396 – 3399; *Angew. Chem.* **2014**, *126*, 3464 – 3467.
[12] Y. Zhang, K. Basu, J. W. Canary, A. Jerschow, *Phys. Chem. Chem. Phys.* **2015**, *17*, 24370 – 24375.
[13] a) D. Moharregh-Khiabani, R. A. Linker, R. Gold, M. Stangel, *Curr. Neuropharmacol.* **2009**, *7*, 60 – 64; b) C. B. Burness, E. D. Deeks, *CNS Drugs* **2014**, *28*, 373 – 387.
[14] a) Z. Rappoport, S. Patai, C. Degani, *J. Chem. Soc.* **1963**, 4513 – 4521; b) Z. Grünbaum, S. Patai, Z. Rappoport, *J. Chem. Soc. B* **1966**, 1133 – 1137.
[15] G. Pileio, *J. Chem. Phys.* **2011**, *134*, 214505.
[16] K. Shirono, T. Morimatsu, F. Takemura, *J. Chem. Eng. Data* **2008**, *53*, 1867 – 1871.

Manuscript received: June 20, 2016
Final Article published: ■■ ▮▮, 2016

COMMUNICATIONS

Y. Zhang, X. Duan, P. C. Soon,
V. Sychrovský, J. W. Canary, A. Jerschow**

■■ – ■■

Limits in Proton Nuclear Singlet-State Lifetimes Measured with *para*-Hydrogen-Induced Polarization

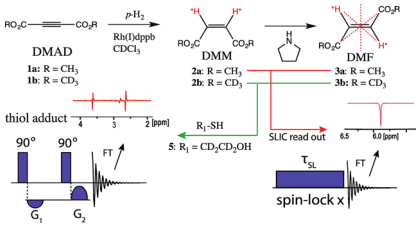

Single for a lifetime: Polarization and the singlet state are preserved over two controlled chemical steps to create long-lived proton singlet states. Owing to the high symmetry, the singlet-state readout requires either a chemical de-symmetrization or a long and repeated spin lock.